iScience

CellPress
OPEN ACCESS

Article

Sensorized objects used to quantitatively study distal grasping in the African elephant

Matteo Lo Preti,
Lucia Beccai

matteo.lopreti@iit.it (M.L.P.)
lucia.beccai@iit.it (L.B.)

Highlights

The tactile interaction of an African elephant is quantified for distal grasping

Two sturdy sensorized objects allow safe measurements with the large mammal

Grasping pressure on the cylinder is finely modulated with the distal trunk

An energy-efficient grasping and lifting behavior is induced by the handle

Lo Preti & Beccai, iScience *26*, 107657
September 15, 2023
https://doi.org/10.1016/j.isci.2023.107657

iScience

CellPress
OPEN ACCESS

Article

Sensorized objects used to quantitatively study distal grasping in the African elephant

Matteo Lo Preti[1,2,*] and Lucia Beccai[1,3,*]

SUMMARY

Nature evolved many ways to grasp objects without using hands: elephants, octopuses, and monkeys use highly dexterous appendices. From a roboticist's perspective, the elephant trunk is a fascinating manipulator, which strategies can empower robots' interaction capabilities. However, quantifying prehensile forces in such large animals in a safe, ethical, and reproducible manner is challenging. We developed two sensorized objects to investigate the grasping of an adult African elephant with deliberately occluded vision. A cylinder and a handle provided a distributed force (80 and 6 taxels) and inertial measurements in real-time, resisting dirt and shocks. The animal curled the distal portion of the trunk to grasp the tools. Using force and contact area data of the cylinder revealed the animal's ability to finely modulate pressure. The handle data provided insights into the energy-efficient behavior of the animal, with no significant grasping force changes despite variations imposed on both weight (5-15 kg) and initial position of the object.

INTRODUCTION

An enormous number of animals without hands show versatile manipulation capabilities, and they rely on their dexterity to feed and survive.[1] Nevertheless, the human hand gives the gold standard for manipulation to date. Grasping an object is the foundation of manipulation, as an animal must establish a stable grip to manipulate it efficiently. This ability differs among species since animals require tactile feedback for manipulation, even with well-developed eyesight.[1] Considering the definition of manipulation as "an agent's control of its environment through selective contact,"[2] the absence of hands does not relate to the lack of manipulation capability.

Many animals possess prehensile appendices. One of the most notable examples is the octopus, a soft-bodied mollusk with eight tapered arms[3,4] with a muscular hydrostat structure.[5] The octopus can modulate its stiffness by exerting great force on its surroundings, actively manipulating items with its arms, or moving over various terrains.[6] In particular, the front arms are mainly used for elongation and grasping, whereas the other arms are devoted to locomotion.[7] The octopus starts contacting an object from the root of its arm and then covers it until its tip makes contact. Then, its arms wrap around the object using numerous suckers for stable grasping. This strategy enables the arm to grasp unknown obstacles without a complex brain signal,[8–10] and the control is delegated to the dynamics of the flexible arm.[11,12]

On land, prehensile appendices often have a skeleton. This applies to a monkey's tail, which functions almost as a dexterous fifth limb and is used for sturdy grasping and body support while moving.[13] Spider monkeys and capuchins have additional muscular development[14] and neural innervation[15] in their tails for strength and sensitivity. However, only capuchins have a dedicated brain region associated with tail control.[15] The tail of spider monkeys has a higher mechanical strength and a more elaborate neural control and tactile sensitivity than capuchins. Spider monkeys rely on prehensile tails to support their body weight[16] and use them in acrobatic movements; hence, the greater development of their neural and tactile abilities.[15] In contrast, the tail of capuchins acts almost like a safety harness.[13] However, it is critical for manipulating difficult-to-reach food items.

Still on land but without a skeleton, the elephant trunk is a large prehensile appendix and a muscular hydrostat. Elephants use it to explore and navigate the world, siphon water, sprinkle dust and mud, snorkel, grasp, and manipulate objects in air and water.[17–19] It can elongate, contract, bend, and twist,[5] and it has a thick layer of skin with wrinkles and folds of different dimensions from the tip to the base of the trunk. The ventral side of the Asian elephant's trunk is robust and somewhat stumpy, and just one finger protrudes from the dorsal side of the tip. In contrast, the African elephant's trunk has two fingers to pinch objects.[20] This versatile organ allows highly sensitive smell and touch perception, guiding a rich set of behaviors.[21–23] Touch is fundamental for sensorimotor coordination. In fact, these animals exhibit exquisite motor control as they can dexterously manipulate delicate objects, wield tools,[24] and handle heavy loads.[25]

The proboscis represents a remarkable natural model for manipulation without hands since it interacts in both a strong and gentle manner with an impressive range of objects. Several experiments have recently focused on studying how the elephant uses the trunk for grasping and investigating the stereotypical motion primitives. For instance, Wu et al. showed that an African elephant can pick up a pile of food by

[1]Soft BioRobotics Perception Lab, Istituto Italiano di Tecnologia, 16163 Genova, Italy
[2]The BioRobotics Institute, Scuola Superiore Sant'Anna, 56025 Pontedera, Italy
[3]Lead contact
*Correspondence: matteo.lopreti@iit.it (M.L.P.), lucia.beccai@iit.it (L.B.)
https://doi.org/10.1016/j.isci.2023.107657

compressing it with its trunk and that it can modulate the force to collect granular materials.[26] The same group studied the strategies implemented by an African elephant to lift weights from 20 kg to 60 kg by wrapping a barbell.[27] Moreover, Dagenais et al. identified the strategies and synergies that two African elephants have evolved to reduce the biomechanical complexity of their trunk.[28] These latter investigations highlight a set of grasping strategies in African elephants, we refer to as "distal grasping". Namely, this indicates that the distal part of the trunk is primarily involved in prehensile tasks, e.g., pinching (with or without using suction) and curling around an object.

Gripping objects with the proper amount of force for lifting them, or the inability to do so, is critical for survival.[29–31] Analyzing the gripping force signals tailored to the trunk movement during task execution can provide unprecedented insights to shed light on the elephant's capability to perform the task. At the same time, understanding the modulation of the gripping forces can help abstract basic principles to design innovative trunk-inspired soft manipulators.[32–34]

However, interaction with such large mammals is risky, and direct measurements (e.g., electrodes[35]) are impossible. Instead, an indirect approach is needed to gather quantitative and reliable information, like using sensorized objects. In the literature, there are limited examples of tools to obtain prehensile force data, and they are devoted to studying the interaction of human and robotic hands with objects. Recently, Cornette et al.[36] developed a wooden box with two protruding load cells to record the pinch force. An apple was released as a reward when the animal pinched the mechanism with variable resistance. Solutions relying on smart garments such as gloves[37,38] are impractical with elephants since they tend to wipe themselves.[28] Altobelli et al.[39] presented two instrumented objects to investigate three-finger human grasp properties. Koiva et al.[40] designed iObject to fit the average human hand, be cable-free, maintain maximum comfort, and measure contact and motion data robustly while being used. In,[41] iObject was used to evaluate the spatial location of the contact points and the magnitude of the forces applied by the human hand to the object. More recently, Gao et al.[42] developed modular sensorized objects for trajectory tracking. Although force sensors are not embedded in these objects, they can facilitate benchmarking the dexterity and performance of artificial hands and grippers.

In this work, we study the African elephant's distal grasping of sensorized objects with deliberately occluded vision to prioritize touch. We developed two objects with the highest probability of being grasped with the distal part of the trunk. Their design was optimized considering the previous study by Dagenais et al. in which various types of non-sensorized objects were used.[28] A sensorized cylinder was developed to obtain a force map and inertial data without compromising maneuverability. Specific soft inductive sensors were designed, built, and integrated to obtain spatial information from eighty taxels. A sensorized handle was developed to gather force and inertial data while modifying its weight without varying the outer shape. Both sensorized objects were designed to be safe for the animal to interact with, operate in real-time in dirty environments, and resist shocks. The behavioral hypothesis for the first experiment was that the elephant would grasp the side of the cylindrical object with the distal portion of the trunk.[28] For the second experiment, we hypothesized that an object with the shape of a handle would induce changes in the applied force or in the grasping strategy when varying its weight and its initial position with respect to the trunk. The results of this study can pave the way for new protocols for animal physical interaction studies, allowing an indirect quantification of tactile-guided grasping capabilities.

RESULTS

An 18-year-old male African elephant named Itzek, living at the ZooSafari Park in Fasano (Italy), was involved in the experimentation. We took measures to avoid the risks related to the experiments, as discussed in the Table 1 and in the STAR Methods. As a result of this analysis, an experimental protocol was defined for the elephant to interact with a sensorized cylinder and a sensorized handle within the setup shown in Figure 1. The two objects are described in the STAR Methods and illustrated in Figures 2 and 3. Video S1 shows an overview of the MATLAB application developed to inspect the trials before selection. After data selection and cleaning, nine trials were analyzed with the cylinder (plus seven additional trials to examine the contact area) and 25 with the handle. Videos S2 and S3 show the operation of the sensorized cylinder and handle, respectively, together with an example of grasping trial for each case.

Sensorized cylinder experiments

The nine selected trials were compared in terms of the duration of contact in the grasping task, i.e., from the time contact was made to the release of the object and in terms of the maximum force exerted by the proboscis. Figure 4A shows that the contact duration ranged between 1.25 s and 2 s, whereas the maximum force ranged from 33 N to 43 N.

The time axes of the trials were normalized to compare the evolution of the force applied to the object. The normalized impulse of the force was then computed by integrating the force value over time and by dividing it by the maximum value:

$$I_n = \frac{\int_0^1 F\,dt}{\max \int_0^1 F\,dt} \qquad \text{(Equation 1)}$$

The impulse of the trials and the average profile are reported in Figure 4B. Around 10% of the maximum force was exerted within the first 35% duration of the grasping task, as highlighted in red in the graph. At that point, the trunk was curled around the cylinder and slightly

Table 1. A comprehensive view of the risk analysis assessment

Identified source of risk	Countermeasures	P	H	R
Object ingestion	• Ropes • Matched size of entrance holes and objects	2	2	4
Object explosion outside the workspace	• Ropes • Matched size of entrance holes and objects • Inner liner to protect from bumps	1	3	3
Object breakage	• Use of plastic materials • First contact after release is made with plastic or more resistant parts • Object replacements	1	1	1
Object manipulated from non-sensorized parts	• Object affordance • Large sensorized areas • Negligible differences in the outcome if the force is not completely captured	2	2	4
Loss of interest	• Food-driven experiments • Interaction with unknown objects	2	3	6
Unsuitable weather	• Coverage to resist light rain	2	3	6
Animal in musth	• Iron experimental setup to resist if hit	4	4	16
Average risk:				7

Sources of risk related to interaction with the sensorized objects and environmental conditions were identified, and possible countermeasures were considered to reduce the risk as low as reasonably practicable. The risk R is the result of the product of the probability P and harm severity H and is classified into minor ($R < 4$), moderate ($4 \leq R < 10$), major ($10 \leq R < 17$), and severe ($R > 17$).

adjusted the contact. A lifting phase then took approximately 55% of the remaining time (green in the graph). During contact and lifting, the standard deviation among trials increased from 0.016 to 0.0830, respectively. In the remaining part of the task (10% of the remaining time, blue part of the figure), the cylinder was released without being thrown abruptly. To investigate the temporal distribution of the applied forces, the contact area was retrieved using a threshold operation to obtain the active taxels. Their number provided a discretization into 80 levels, multiplied by the area of the taxel. Figure 4C shows the evolution over time of the contact area for the trials and the average value with standard error. The values range from 56 cm^2 to 94 cm^2 (see Figure 4D). It should be noted that such evolution follows that of the force. In fact, the applied pressure is almost constant across the trials, as highlighted in Figure 4C.

Then, the spatial distribution of the applied forces was analyzed. The 8x10 force mapping matrix was obtained for each trial when the trunk exerted the maximum force. The matrix for each trial was treated as an image. Variations in the grasping orientation due to the axial symmetry of the cylinder were compensated using a tactile image alignment algorithm, whose pseudocode is reported as algorithm 1. The resulting images are shown in Figure S3C. The structural similarity index[43] was calculated for each pair of aligned images. Figure 4E shows the high variability among trials; in particular, trials 2 and 11 are the least similar to the others. However, the overall shape of the area most likely to be touched could be estimated, as reported in the unwrapped cylinder surface in Figure 4D.

Sensorized handle experiments

The elephant showed the same behavior for both trials related to grasping the object in the near and middle positions of the setup, with the curling movement shown in Figure 5. Hence, these two locations are shown for comparison when varying the weights.

Figure 5A shows the time duration of the trials from object pick-up to release, the maximum force, maximum acceleration of the handle, and the holding time at a high force level. The average value was calculated by considering all the possible trials. The duration ranges from 1.4 s to 2.3 s; the maximum force ranges from 22 N to 50 N, the maximum acceleration ranges from 3 ms^{-2} to 29 ms^{-2}, and the holding time from 0.03 s to 0.65 s.

The effect of weight on the duration is a slight increase in the variability among trials, without a significant impact on the average value that does not show high fluctuations. Table 2 provides a summary of the trials with the sensorized handle having as starting position the close and the middle location. The duration of the task was almost the same in the two cases.

The prehensile force exerted when the object was positioned closer to the setup wall, i.e., when the trunk did not have to elongate to reach the object, is 10N higher than when the object was at the middle position, with a 25% increment in the holding time. No noticeable trends related to weight variation were observed. Conversely, the recorded acceleration was half in the trials with the handle starting position in the middle.

Following an analogous procedure used for the cylinder, the time axes of the trials were normalized. Then, the normalized impulse of the force was computed by using Equation 1. The average impulse profile when changing the weight and object starting positions are reported in Figure 5B. The profiles in the first two locations show many similarities, reflecting that the elephant behaved similarly. The force is applied more abruptly to the cylinder in the close position, and the plateau is reached sooner than in the middle case. The peaks in the force are also less regular. The far position subserved a shift in the grasping type. In this case, the object's distance prevented the elephant from curling around it. The alternative action was to take the object between the two fingertips and pull it

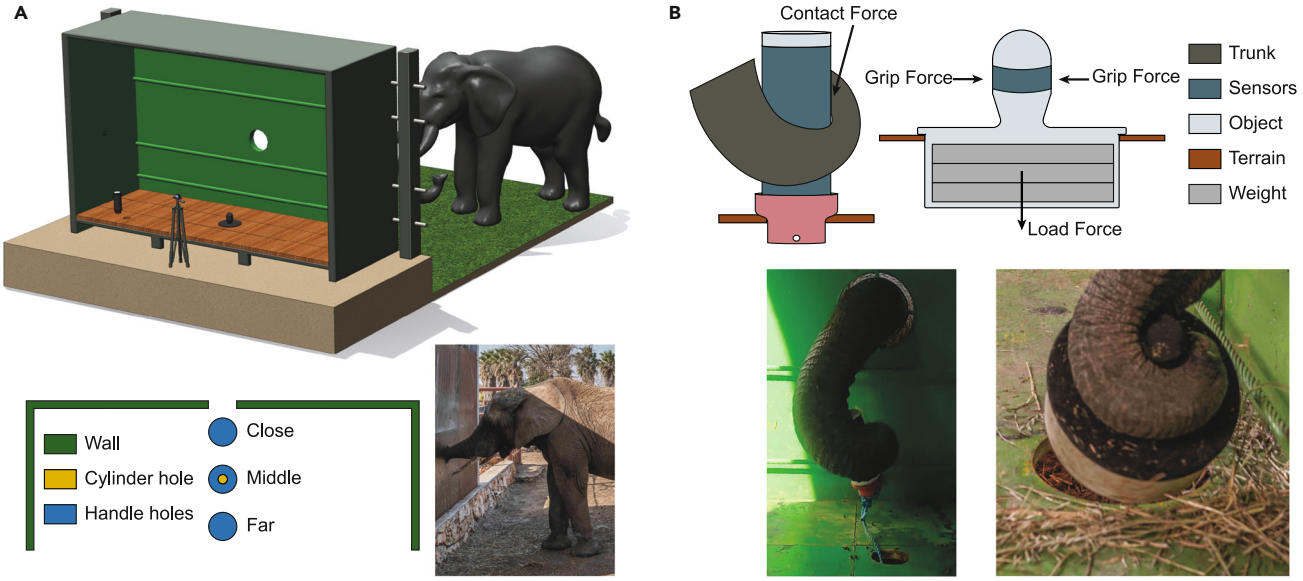

Figure 1. Experimental setup and protocol

The pictures in the bottom part of the panel show Itzek, a male individual of *L. Africana*, ZooSafari (Fasano, Italy).

(A) 3D sketch of the experimental setup and top view showing the locations of the holes.

(B) The protocols for the experiments with the cylinder and the handle.

from the ground hole. However, after this action, the animal could not easily reach the food underneath the object and soon lost interest in the task.

The object's orientation during grasping can be considered to analyze and understand the grasping strategy used by the elephant in this case. Figure 5C shows the force and angular data of three trials as an example. In one scenario (top graph), the handle is slightly adjusted and rotated up to 90° and then rotated about the z axis. In the second scenario (middle graph), the handle is somewhat adjusted and rotated up to 90°, then it is roto-translated about the z axis. In a final scenario, the handle is slightly adjusted and rotated up to 90° and then translated toward the opening of the setup.

The expected movement is shown in a 2D simplified scenario in Figure 5D (Lift). In fact, the elephant was expected to pick the object up vertically by balancing its weight to break the static equilibrium. Instead, the behavior observed is reproduced in Figure 5D (Tilt). The no-slip condition was assumed between the trunk and the handle to evaluate the force the animal uses to break the static equilibrium.

In the case of object lifting (Figure S4A), the handle can be detached from the ground by applying a vertical force F_L, such that:

$$F_L \geq mg \qquad \text{(Equation 2)}$$

Considering the tilting task implemented by the trunk (Figure S4B), a force F_T is applied such that the object cannot rotate counterclockwise. The minimum force necessary to turn the body clockwise is given by the balance of the momentum about the Center of Mass (CoM). This force can be compared to F_L, which is the minimum force necessary to start the motion of the handle during lifting.

$$\begin{cases} F_x = R_x \\ F_y = W - R_y \\ F_y = F_T \sin\alpha \\ F_x = F_T \cos\alpha \\ \sum_i M_{O,i} \geq 0 \end{cases} \Rightarrow \begin{cases} F_x = R_x = F\cos\alpha \\ F_y = F\sin\alpha \\ R = W - F\sin\alpha \\ b_{F_y}F_y + b_{F_x}F_x - b_w W - b_{R_y}R_y - b_{R_x}R_x \geq 0 \end{cases} \qquad \text{(Equation 3)}$$

$$b_{F_y}\sin\alpha\, F_T + b_{F_x}\cos\alpha F_T - b_W W - b_{R_y}(W - F_T\sin\alpha) - b_{R_x}\cos\alpha F_T \geq 0 \qquad \text{(Equation 4)}$$

Leading to:

$$\frac{>0\,\forall\,\alpha\in[0,\pi/2]}{\left((b_{Fy}+b_{Ry})\sin\alpha+(b_{Fx}-b_{Rx})\cos\alpha\right)F_T \geq (b_W+b_{R_y})W} \qquad \text{(Equation 5)}$$

$$F_T \geq \left(\frac{b_W+b_{Ry}}{(b_{Fy}+b_{Ry})\sin\alpha+(b_{Fx}-b_{Rx})\cos\alpha}\right) m\,g \qquad \text{(Equation 6)}$$

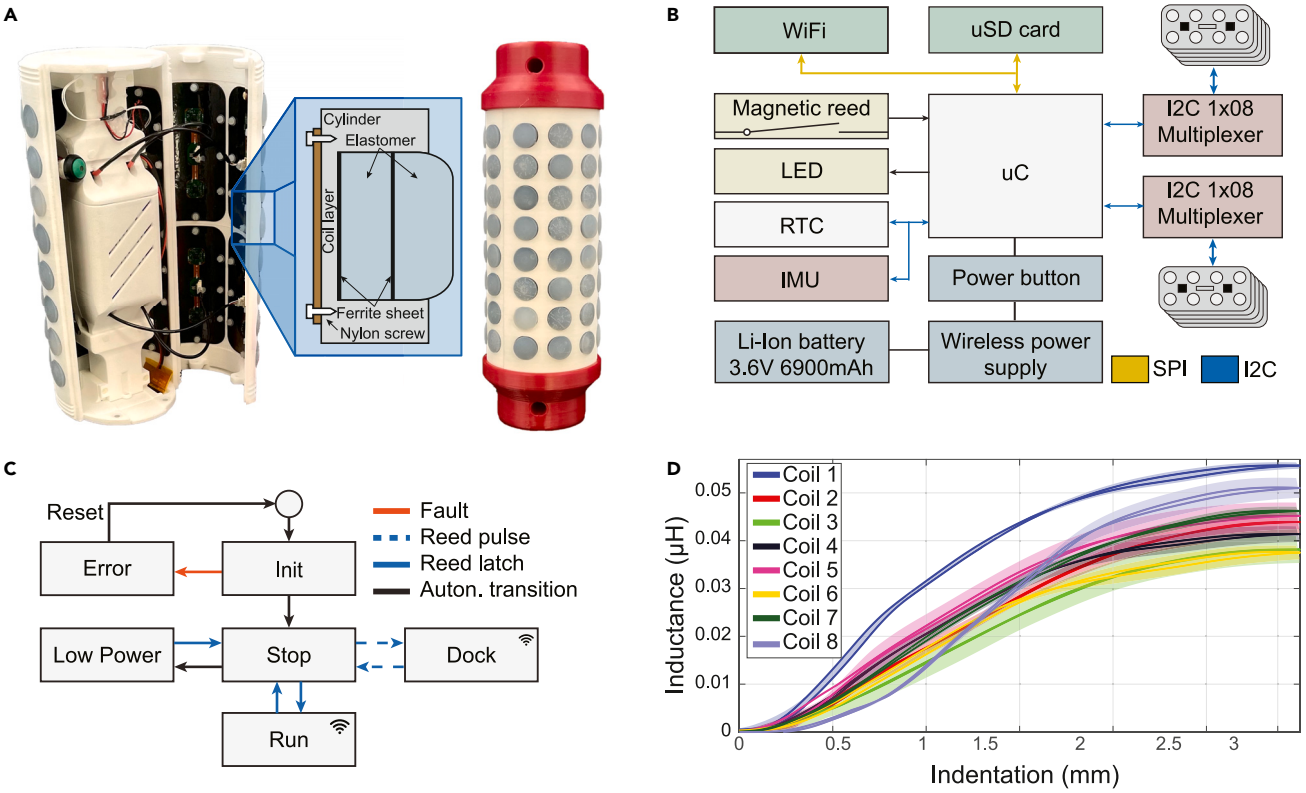

Figure 2. Characteristics of the sensorized cylinder

(A) Sensorized cylinder with the slot open to access the power button and the internal electronics and closed with the side protection inserted, with an inset containing the sketched section of the sensor.

(B) Block diagram of the electronic components.

(C) State chart of the device.

(D) Responses of the eight coils of one of the ten 8-coil PCBs.

By substituting the dimensions of the handle reported on Figure S4C:

$$F_T \geq \left(\frac{155}{197\cos\alpha + 89\sin\alpha}\right) m\,g \qquad \text{(Equation 7)}$$

Hence, the force ratio in percentage is:

$$\frac{\Delta F}{F_L} = 100\left(\frac{F_T}{F_L} - 1\right) = 100\left(\frac{155}{197\cos\alpha + 89\sin\alpha} - 1\right) \qquad \text{(Equation 8)}$$

The tilting behavior needs less force for $\alpha < 68°$. In the best-case scenario, i.e., $\alpha \approx 24°$, the net force saved is 28% with respect to lifting.

DISCUSSION

Animals have evolved their prehensile organs to facilitate foraging, and mechanosensory adaptation is crucial for this task since it enhances active exploration and object recognition.[44] Elephants seem to have most of the "neural attention" focused on their trunk. In fact, their retinal ganglion cells are concentrated in the upper temporal region, corresponding to the area of the visual field where the trunk moves.[45] Most recent studies show how the motor strategy in African elephants depends on a finger "motor foveae" and on a positional bias of neurons toward the trunk tip representation in their facial nuclei.[46] The results of this study support earlier suggestions regarding tactile foveation, which refers to a tactile fovea that would permit greater somatic information during probing and exploration.[47] The elephant brain is the least well-developed for sight compared to the other four senses.[23] This study further prioritized touch by occluding the elephant's vision during distal grasping.

The sensorized cylinder and handle used in the two weeks of experiments underwent repeated shocks but without any damage. Although three copies of each object were fabricated, only one was used. The elephant tolerated the chosen geometry and materials, and the objects were used in an unstructured environment to reliably gather tactile and inertial data. No training was performed before the experimental time window since Itzek was naturally inclined to explore unknown objects and interacted willingly.

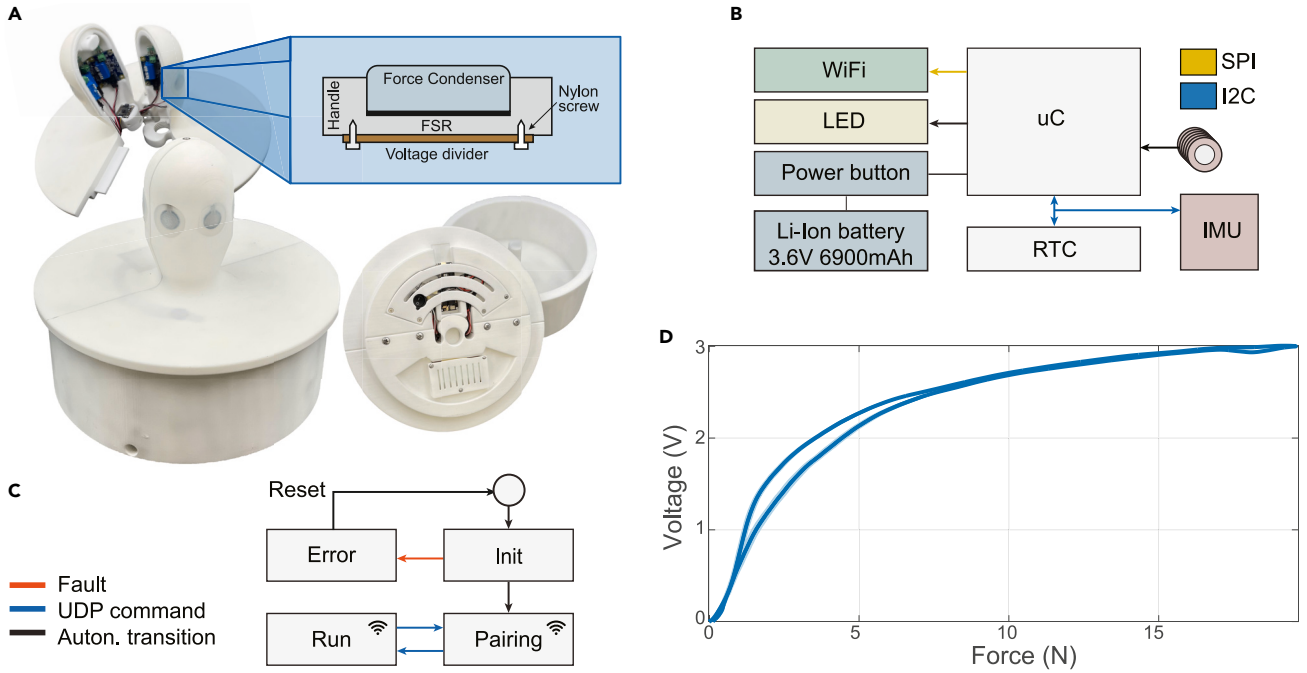

Figure 3. Characteristics of the sensorized handle

(A) Sensorized handle separated from the weight holder to access the power button and the internal electronics, with the two-halves separated and closed. The inset shows a sketch of the sensor's section.

(B) Block diagram of the electronic components.

(C) Device states.

(D) Response of one of the six taxels.

Regarding the interaction with the sensorized cylinder, our results show that the elephant performed distal curling with precise pressure control without damaging the object, confirming our behavioral hypothesis. Indeed, this exemplar could, in principle, exert large forces, e.g., to break a tree branch. Even though each elephant individual has peculiar characteristics, stereotypical behaviors are shared and can be inducted or derive from the environment. This was evident when he was tired, or the weather was too cold. Our experimental sessions were arranged to avoid these circumstances. According to the experienced keepers of the ZooSafari, cold or windy weather can affect the behavior of all the elephants they take care of, particularly their will to interact with them. In these large mammals, such conditions can increase the probability of abrupt use of their incredible force.

The contact probability maps were matched to the corresponding videos for the selected trials. From this analysis, it can be inferred that the trunk area effectively in contact with the cylindrical target was lower than 100 cm^2 and was located at its ventral side. Depending on the object's size, the contact location shifts toward the proximal part of the trunk.[28] The pivotal point thus shifts so that the momentum decreases. This suggests that tactile mechanoreceptors in the ventral skin may be the key to understanding how forces are so finely controlled during all the grasping phases.

Concerning the manipulation of the sensorized handle, the aim was to investigate how the continuum arm of the elephant modified its planning and strategy when picking up objects of different weights from different distances. The results of the interaction were, however, unexpected. On the one hand, after a few trials, the elephant changed the motion planning immediately after distally grasping the object. He relied on the lever mechanism to move the object on the ground without lifting it, which was shown to be more efficient from an energetic point of view. On the other hand, the maximum force applied did not vary significantly for the configurations tested in which both the starting object position and object weight varied. Because of the limited number of trials, any statistical analysis on different weights would not have had enough statistical power. Hence, the differences between close and middle positions were analyzed. The limited range of weights (5 kg–15 kg), chosen following the safety protocols at the ZooSafari, may have affected the grasping behavior since the elephant showed no change in grasping force. Further studies with a wider set of weights may explain this aspect in more detail. The elephant relied on distal curling for every configuration, except when the object was too far away for him to wrap his trunk. However, positioning the object at a far distance did not elicit the pinching strategy, and he quickly lost interest.

In principle, to focus the investigation on pinching, the experimental protocol could be revised by selecting appropriate object dimensions, the initial position on the ground, and weights. In order to grab an object, an animal must "build" a model of the environment, plan an effective action, and finally assess the outcome. Living organisms possess ingenious and efficient closed-loop control since they rely on their response to somatosensory triggers to survive. They integrate multiscale structures and multi-modules while maintaining their

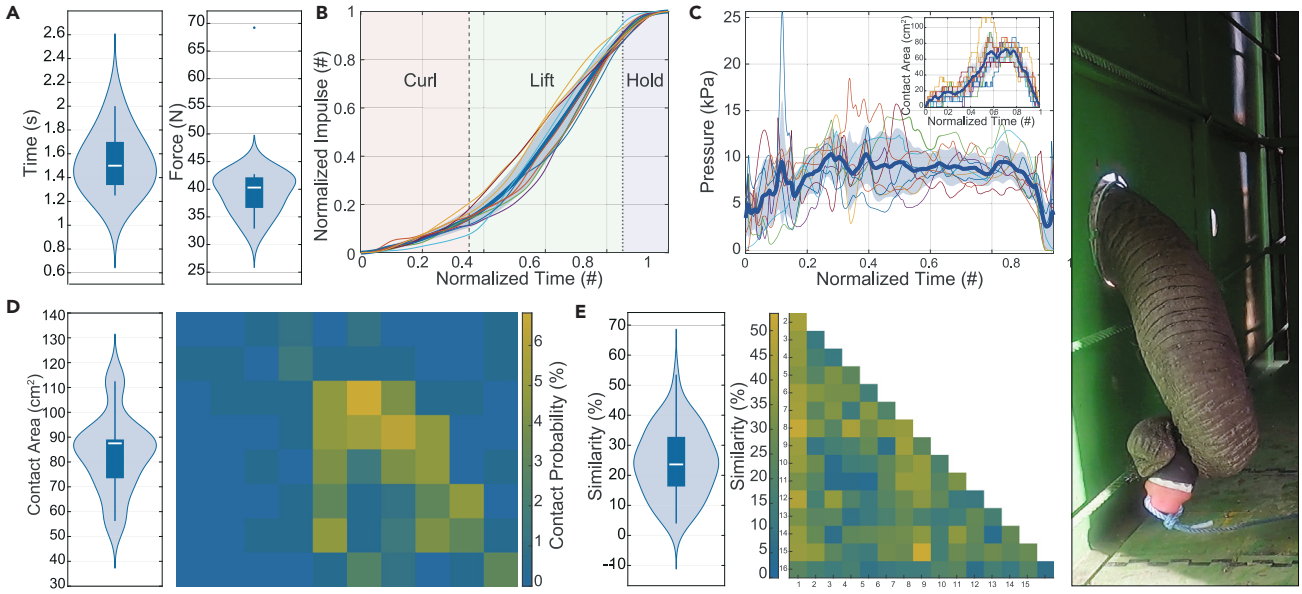

Figure 4. Results of the experiments with the sensorized cylinder, with a typical curling grasp depicted on the right

(A) Boxplot of time and force variability among the selected trials, with shaded violin plot.

(B) Normalized impulse of the selected trials and average profile (thicker blue line) of the grasping activity. Around 10% of the maximum force was exerted in the first 35% of the grasping task (red part of the figure), when the trunk curls around the object placed on the ground, whereas the following lifting phase took nearly 55% of the remaining time (highlighted in green), and a final holding phase is shown in blue.

(C) Evolution of the applied pressure over time, with the contact area shown in the inset. The blue line represents the average value, and the blue shaded area is the blue standard error.

(D) Variability of the contact area among the trials and the probability of each tactile element (taxel) being touched during the grasping, shown in the unwrapped cylinder surface.

(E) Similarity of the contact area shape among trials.

structural identity.[48] A closed loop is necessary in the artificial world to obtain autonomy and interaction capabilities in a dynamic environment.[49]

Nevertheless, obtaining highly integrated and autonomous bio-inspired robots is still enormously challenging,[50] and radical innovations are needed to design systems that can efficiently deal with the world's complexity and uncertainty.[51] Theories and findings on manipulation without hands can help us gain more general insights into how animals interact with the physical world[1] and enable us to explore paradigms other than the human arm-hand system. We believe that the use of sensorized objects to quantify distal grasping is a pivotal step toward abstracting engineering principles from the trunk's capabilities, which are just starting to be unveiled.

Limitations of the study

This research defined a methodology to obtain quantitative data about interactions with objects from a large mammal, like the elephant. It contributed to such a poorly explored multidisciplinary field by providing safe tools for both the elephant and the researcher. The developed

Algorithm 1. Pseudo-code for the contact map alignment. A target image is matched with replicated and rotated versions of the other images. When the configuration that minimizes the unpredictability of the grasping is found, the structural similarity index is calculated for each pair of aligned images.

Select the target image *TargetImg*
FOR each other image *Img* DO
    Calculate *RepImg* by replicating *Img* three times horizontally and vertically
    FOR each angle $\alpha = 0 : 5 : 355$ DO
        Calculate *RotImg* by rotating *RepImg* by α
        Calculate the cross-correlation *ccr* between *RotImg* and *TargetImg*
    Chose the image *SelImg* that maximizes the cross-correlation
FOR each pair of *SelImg* DO
    Calculate the Structural Similarity Image.

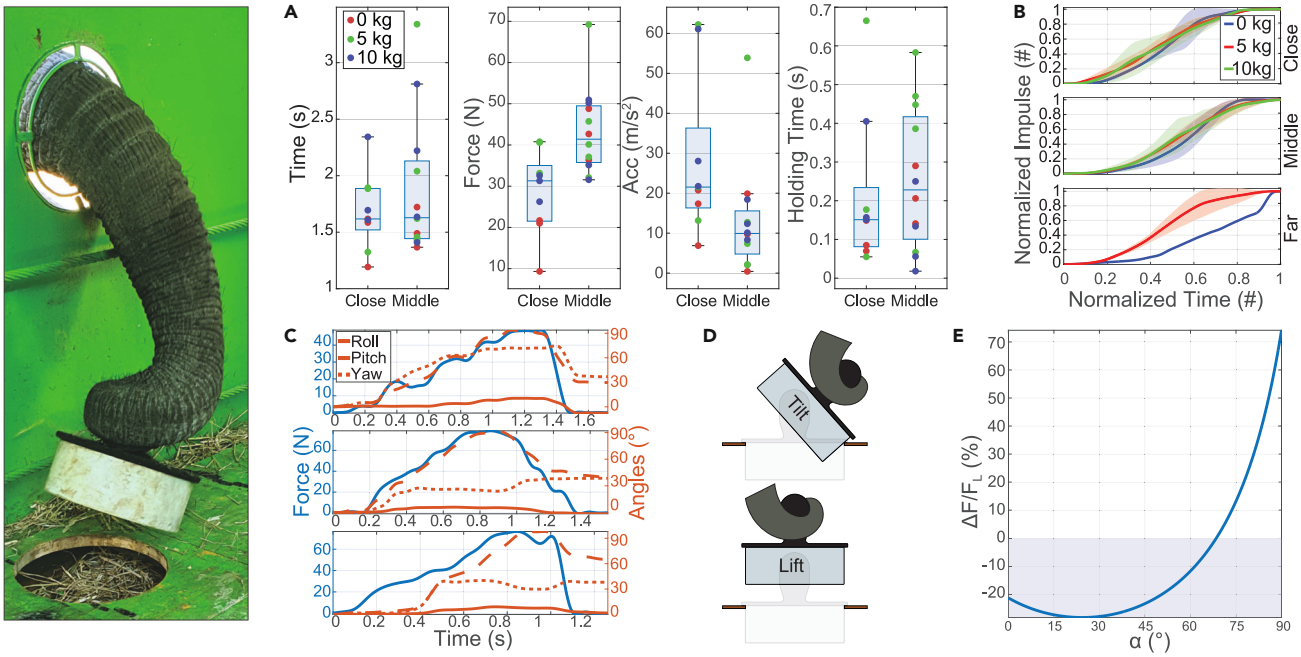

Figure 5. Results of the experiments with the sensorized handle, with a typical curling grasp depicted on the left

(A) Variability of the trial duration, applied force, acceleration, and holding time when varying the weight of the handle and its starting position. Value for 0, 5, and 10kg trials are reported in red, green, and blue, respectively. The boxplot of the overall distribution is shown for comparison.

(B) Normalized impulse of the grasping activity for different locations and weights of the handle.

(C) Examples of force and angle evolution over time in three trials.

(D and E) Sketch of the prehensile strategy in the two cases of lift and tilt, and (E) percentage force used by tilting with respect to lifting while varying the angle of application of the force.

methods *per se* can undergo further refinement, development, and generalization. The constraints of the study derive both from the availability of resources at ZooSafari, and from the limited time available on a daily basis to involve the animal in the experiments without affecting his enrichment activities. This limited the amount of data that could be collected and any statistical analysis. Furthermore, the absence of initial training required a substantial amount of time dedicated to tune the experimental protocol to increase the likelihood of the elephant interacting with the objects.

STAR★METHODS

Detailed methods are provided in the online version of this paper and include the following:

- KEY RESOURCES TABLE
- RESOURCE AVAILABILITY
  - Lead contact
  - Materials availability
  - Data and code availability
- EXPERIMENTAL MODEL AND SUBJECT DETAILS

Table 2. Summary of the compared features (task duration, maximum force, maximum acceleration, and holding time) among trials performed with the sensorized handle, positioned at the close and middle location

	Close	Middle
Time (s)	1.62 (0.37)	1.63 (0.69)
Force (N)	31.31 (13.50)	41.40 (13.74)
Acceleration (m/s^2)	21.53 (19.99)	9.93 (10.80)
Holding time (s)	0.15 (0.15)	0.23 (0.32)

Median values are reported with the interquartile range between brackets.

- METHOD DETAILS
  - Experimental setup and protocol
  - Sensorized cylinder
  - Sensorized handle
  - Data selection and cleaning
- QUANTIFICATION AND STATISTICAL ANALYSIS

SUPPLEMENTAL INFORMATION

Supplemental information can be found online at https://doi.org/10.1016/j.isci.2023.107657.

ACKNOWLEDGMENTS

This work received funding from the European Union's Horizon 2020 research and innovation program under grant agreement No. 863212 (PROBOSCIS project). We thank Fabio Rausa, director of the ZooSafari (Fasano, Italy) for his support in establishing the collaboration, and the experts of the safari park, Maik Hones and Matteo Legrottaglie, for their help in defining a safe and ethical experimental protocol, and for their support during the elephant experiments. We would like to thank Enrico Donato, Camilla Agabiti, and Egidio Falotico from Scuola Superiore Sant'Anna for the discussions while designing the experiments. From Istituto Italiano di Tecnologia, we express our thanks to Mirco Di Salvo, Claudio Lorini, and Simone Lantean for their help in the development of the sensorized cylinder, Seonggun Joe for the initial discussions to define the experimental protocols, and Irene Bernardeschi for identifying the suitable safari park for performing experiments.

AUTHOR CONTRIBUTIONS

Conceptualization, L.B. and M.L.P.; Methodology, L.B. and M.L.P.; Software, M.L.P.; Formal analysis, M.L.P.; Investigation, L.B. and M.L.P.; Resources, L.B. and M.L.P.; Data Curation, M.L.P.; Visualization, M.L.P.; Writing – Original Draft, M.L.P.; Writing – Review & Editing, M.L.P. and L.B.; Funding Acquisition, L.B.; Supervision, L.B.

DECLARATION OF INTERESTS

The authors declare no competing interests.

INCLUSION AND DIVERSITY

We support inclusive, diverse, and equitable conduct of research.

Received: February 10, 2023
Revised: June 23, 2023
Accepted: August 15, 2023
Published: September 7, 2023

REFERENCES

1. Sugasawa, S., Webb, B., and Healy, S.D. (2021). Object manipulation without hands. Proc. Biol. Sci. *288*, 20203184.
2. Mason, M.T. (2018). Toward Robotic Manipulation. Annu. Rev. Control Robot. Auton. Syst. *1*, 1–28. https://doi.org/10.1146/annurev-control-060117-104848.
3. Kier, W.M., and Stella, M.P. (2007). The arrangement and function of octopus arm musculature and connective tissue. J. Morphol. *268*, 831–843.
4. Kennedy, E.B.L., Buresch, K.C., Boinapally, P., and Hanlon, R.T. (2020). Octopus arms exhibit exceptional flexibility. Sci. Rep. *10*, 20872.
5. Kier, W.M., and Smith, K.K. (1985). Tongues, tentacles and trunks: the biomechanics of movement in muscular-hydrostats. Zool. J. Linn. Soc. *83*, 307–324.
6. Mazzolai, B., Margheri, L., Cianchetti, M., Dario, P., and Laschi, C. (2012). Soft-robotic arm inspired by the octopus: II. From artificial requirements to innovative technological solutions. Bioinspiration Biomimetics *7*, 025005.
7. Cianchetti, M., Calisti, M., Margheri, L., Kuba, M., and Laschi, C. (2015). Bioinspired locomotion and grasping in water: the soft eight-arm OCTOPUS robot. Bioinspiration Biomimetics *10*, 035003.
8. Sumbre, G., Gutfreund, Y., Fiorito, G., Flash, T., and Hochner, B. (2001). Control of octopus arm extension by a peripheral motor program. Science *293*, 1845–1848.
9. Yekutieli, Y., Flash, T., and Hochner, B. (2009). Biomechanics: hydroskeletal. Encyclopedia of neuroscience *2*, 189–200.
10. Gutfreund, Y., Flash, T., Fiorito, G., and Hochner, B. (1998). Patterns of arm muscle activation involved in octopus reaching movements. J. Neurosci. *18*, 5976–5987.
11. Kuroe, S., and Ito, K. (2012). Autonomous control of octopus-like manipulator using reinforcement learning. In Distributed Computing and Artificial Intelligence (Springer), pp. 553–556.
12. Ito, K., and Hagimori, S. (2017). Flexible manipulator inspired by octopus: development of soft arms using sponge and experiment for grasping various objects. Artif. Life Robot. *22*, 283–288.
13. Garber, P.A., and Rehg, J.A. (1999). The ecological role of the prehensile tail in white-faced capuchins (Cebus capucinus). Am. J. Phys. Anthropol. *110*, 325–339.
14. Organ, J.M., Muchlinski, M.N., and Deane, A.S. (2011). Mechanoreceptivity of prehensile tail skin varies between ateline and cebine primates. Anat. Rec. *294*, 2064–2072.
15. Rosenberger, A.L. (1983). Tale of tails: parallelism and prehensility. Am. J. Phys. Anthropol. *60*, 103–107.
16. Cant, J.G. (1986). Locomotion and feeding postures of spider and howling monkeys: field study and evolutionary interpretation. Folia Primatol. *46*, 1–14.
17. Rasmussen, L.E.L., and Munger, B.L. (1996). The sensorineural specializations of the trunk tip (finger) of the Asian elephant, Elephas maximus. Anat. Rec. *246*, 127–134. https://doi.org/10.1002/(SICI)1097-0185(199609)246:1<127::AID-AR14>3.0.CO;2-R.
18. Chevalier-Skolnikoff, S., and Liska, J. (1993). Tool use by wild and captive elephants. Anim. Behav. *46*, 209–219. https://doi.org/10.1006/anbe.1993.1183.
19. Plotnik, J.M., Brubaker, D.L., Dale, R., Tiller, L.N., Mumby, H.S., and Clayton, N.S. (2019). Elephants have a nose for quantity. Proc.

Natl. Acad. Sci. USA *116*, 12566–12571. https://doi.org/10.1073/pnas.1818284116.
20. Shoshani, J.H. (1997). What can make a four-ton mammal a most sensitive beast? Nat. Hist. *106*, 36–44.
21. Plotnik, J.M., Pokorny, J.J., Keratimanochaya, T., Webb, C., Beronja, H.F., Hennessy, A., Hill, J., Hill, V.J., Kiss, R., Maguire, C., et al. (2013). Visual cues given by humans are not sufficient for Asian elephants (Elephas maximus) to find hidden food. PLoS One *8*, e61174.
22. Plotnik, J.M., Shaw, R.C., Brubaker, D.L., Tiller, L.N., and Clayton, N.S. (2014). Thinking with their trunks: elephants use smell but not sound to locate food and exclude nonrewarding alternatives. Anim. Behav. *88*, 91–98.
23. Garstang, M. (2015). The Sensory Environment of Elephants. In Elephant Sense and Sensibility, S. Garstang, ed. (Elsevier), pp. 97–101. https://doi.org/10.1016/B978-0-12-802217-7.00013-2.
24. Hart, B.L., Hart, L.A., and Pinter-Wollman, N. (2008). Large brains and cognition: where do elephants fit in? Neurosci. Biobehav. Rev. *32*, 86–98.
25. Dehnhardt, G., Friese, C., and Sachser, N. (1997). Sensitivity of the trunk of Asian elephants for texture differences of actively touched objects. Zeitschrift fur Saugetierkunde, 37–39.
26. Wu, J., Zhao, Y., Zhang, Y., Shumate, D., Braccini Slade, S., Franklin, S.V., and Hu, D.L. (2018). Elephant trunks form joints to squeeze together small objects. J. R. Soc. Interface *15*, 20180377. https://doi.org/10.1098/rsif.2018.0377.
27. Schulz, A.K., Reidenberg, J.S., Ning Wu, J., Ying Tang, C., Seleb, B., Mancebo, J., Elgart, N., and Hu, D.L. (2023). Elephant trunks use an adaptable prehensile grip. Bioinspiration Biomimetics *18*, 026008. https://doi.org/10.1088/1748-3190/acb477.
28. Dagenais, P., Hensman, S., Haechler, V., and Milinkovitch, M.C. (2021). Elephants evolved strategies reducing the biomechanical complexity of their trunk. Curr. Biol. *31*, 4727–4737.e4.
29. Krebs, J.R., Erichsen, J.T., Webber, M.I., and Charnov, E.L. (1977). Optimal prey choice in the great tit. Anim. Behav. *25*, 30–38.
30. Charnov, E.L. (1976). Optimal foraging: attack strategy of a mantid. Am. Nat. *110*, 141–151.
31. Le Brazidec, M., Herrel, A., Thomas, P., Grégoire, B.A., Aujard, F., and Pouydebat, E. (2017). How aging affects grasping behavior and pull strength in captive gray mouse lemurs (Microcebus murinus). Int. J. Primatol. *38*, 1120–1129.
32. Hannan, M.W., and Walker, I.D. (2001). Analysis and experiments with an elephant's trunk robot. Adv. Robot. *15*, 847–858. https://doi.org/10.1163/156855301317198160.
33. Liu, Y., Ge, Z., Yang, S., Walker, I.D., and Ju, Z. (2019). Elephant's Trunk Robot: An Extremely Versatile Under-Actuated Continuum Robot Driven by a Single Motor. J. Mech. Robot. *11*. https://doi.org/10.1115/1.4043923.
34. Hannan, M.W., and Walker, I.D. (2003). Kinematics and the implementation of an elephant's trunk manipulator and other continuum style robots. J. Rob. Syst. *20*, 45–63. https://doi.org/10.1002/rob.10070.
35. Johansson, R.S., and Westling, G. (1991). Afferent signals during manipulative tasks in humans. In Information Processing in the Somatosensory System (Springer), pp. 25–48.
36. Cornette, R., Delapré, A., Houssin, C., Mulot, B., and Pouydebat, E. (2022). Measuring the force of the tip of the elephants trunk. MethodsX *9*, 101896. https://doi.org/10.1016/j.mex.2022.101896.
37. Dipietro, L., Sabatini, A.M., and Dario, P. (2008). A survey of glove-based systems and their applications. IEEE Trans. Syst. Man Cybern. C *38*, 461–482.
38. Steffen, J.F. (2010). Structured Manifolds for Motion Production and Segmentation: A Structured Kernel Regression Approach.
39. Altobelli, A. (2016). Sensorized Object Approach BT - Haptic Devices for Studies on Human Grasp and Rehabilitation. In Springer Series on Touch and Haptic Systems, A. Altobelli (Springer International Publishing), pp. 21–41. https://doi.org/10.1007/978-3-319-47087-0_3.
40. Koiva, R., Haschke, R., and Ritter, H. (2011). Development of an intelligent object for grasp and manipulation research. In 2011 15th International Conference on Advanced Robotics (ICAR) (IEEE), pp. 204–210.
41. Roa, M.A., Koiva, R., and Castellini, C. (2012). Experimental evaluation of human grasps using a sensorized object. In 2012 4th IEEE RAS & EMBS International Conference on Biomedical Robotics and Biomechatronics (BioRob) (IEEE), pp. 1662–1668.
42. Gao, G., Gorjup, G., Yu, R., Jarvis, P., and Liarokapis, M. (2020). Modular, accessible, sensorized objects for evaluating the grasping and manipulation capabilities of grippers and hands. IEEE Rob. Autom. Lett. *5*, 6105–6112.
43. Wang, Z., Bovik, A.C., Sheikh, H.R., and Simoncelli, E.P. (2004). Image quality assessment: from error visibility to structural similarity. IEEE Trans. Image Process. *13*, 600–612.
44. Catania, K.C. (2012). Tactile sensing in specialized predators–from behavior to the brain. Curr. Opin. Neurobiol. *22*, 251–258.
45. Stone, J., and Halasz, P. (1989). Topography of the retina in the elephant Loxodonta africana. Brain Behav. Evol. *34*, 84–95.
46. Kaufmann, L.V., Schneeweiß, U., Maier, E., Hildebrandt, T., and Brecht, M. (2022). Elephant facial motor control. Sci. Adv. *8*, eabq2789. https://doi.org/10.1126/sciadv.abq2789.
47. Hoffmann, J.N., Montag, A.G., and Dominy, N.J. (2004). Meissner corpuscles and somatosensory acuity: the prehensile appendages of primates and elephants. Anat. Rec. A Discov. Mol. Cell Evol. Biol. *281*, 1138–1147.
48. Egan, P., Sinko, R., LeDuc, P.R., and Keten, S. (2015). The role of mechanics in biological and bio-inspired systems. Nat. Commun. *6*, 7418–7512.
49. Kaspar, C., Ravoo, B.J., van der Wiel, W.G., Wegner, S.V., and Pernice, W.H.P. (2021). The rise of intelligent matter. Nature *594*, 345–355.
50. Ren, L., Li, B., Wei, G., Wang, K., Song, Z., Wei, Y., Ren, L., and Liu, Q. (2021). Biology and bioinspiration of soft robotics: Actuation, sensing, and system integration. iScience *24*, 103075. https://doi.org/10.1016/j.isci.2021.103075.
51. Laschi, C., Mazzolai, B., and Cianchetti, M. (2016). Soft robotics: Technologies and systems pushing the boundaries of robot abilities. Sci. Robot. *1*, eaah3690.
52. Soppelsa, J., Pouydebat, E., Lefeuvre, M., Mulot, B., Houssin, C., and Cornette, R. (2022). The relationship between distal trunk morphology and object grasping in the African savannah elephant (Loxodonta africana). PeerJ *10*, e13108.
53. Lefeuvre, M., Gouat, P., Mulot, B., Cornette, R., and Pouydebat, E. (2020). Behavioural variability among captive African elephants in the use of the trunk while feeding. PeerJ *8*, e9678. https://doi.org/10.7717/peerj.9678.
54. Jolly, A. (1964). Prosimians' manipulation of simple object problems. Anim. Behav. *12*, 560–570.
55. Garvey, P.R., and Lansdowne, Z.F. (1998). Risk matrix: an approach for identifying, assessing, and ranking program risks. Air Force J. Logist. *22*, 18–21.
56. International Organization for Standardization (2016). Occupational Health and Safety Management Systems—Requirements with Guidance for Use (ISO/DIS Standard No. 45001).
57. Rees, P.A. (2004). Low environmental temperature causes an increase in stereotypic behaviour in captive Asian elephants (Elephas maximus). J. Therm. Biol. *29*, 37–43. https://doi.org/10.1016/j.jtherbio.2003.10.004.
58. Wang, H., Liu, Y., Li, W., and Feng, Z. (2014). Design of ultrastable and high resolution eddy-current displacement sensor system. In IECON 2014 - 40th Annual Conference of the IEEE Industrial Electronics Society, pp. 2333–2339. https://doi.org/10.1109/IECON.2014.7048828.
59. Wang, H., Kow, J., Raske, N., De Boer, G., Ghajari, M., Hewson, R., Alazmani, A., and Culmer, P. (2018). Robust and high-performance soft inductive tactile sensors based on the Eddy-current effect. Sens. Actuators A Phys. *271*, 44–52.

STAR★METHODS

KEY RESOURCES TABLE

REAGENT or RESOURCE	SOURCE	IDENTIFIER
Deposited data		
Raw force and inertial data	This paper	https://doi.org/10.17632/9gtwdmyyb9.1
Preprocessed data	This paper	https://doi.org/10.17632/9gtwdmyyb9.1
Data analysis code	This paper	https://doi.org/10.17632/9gtwdmyyb9.1
Experimental models: Organisms/strains		
One adult male elephant *L. africana*	https://zoosafari.it	N/A
Software and algorithms		
MATLAB	https://www.mathworks.com/products/matlab.html	N/A
NI LabVIEW	https://www.ni.com/it-it/shop/software/products/labview.html	N/A

RESOURCE AVAILABILITY

Lead contact

Further information and requests for resources should be directed to and will be fulfilled by the lead contact, Lucia Beccai (lucia.beccai@iit.it).

Materials availability

This study did not generate new materials.

Data and code availability

- Raw data have been deposited at Mendeley Data and are publicly available as of the date of publication. DOIs are listed in the key resources table.
- All original code has been deposited at Mendeley Data and are publicly available as of the date of publication. DOIs are listed in the key resources table.
- Any additional information required to reanalyze the data reported in this paper is available from the lead contact upon request.

EXPERIMENTAL MODEL AND SUBJECT DETAILS

One adult male African elephant (Loxodonta africana) was involved in the experiments with the sensorized objects. All experiments have been approved by the director, veterinarians, and keepers at ZooSafari and performed under the supervision of the keepers.

METHOD DETAILS

The experiments were carried out in January 2022 at the ZooSafari Park in Fasano (Puglia, Italy) with one 18-year-old male individual named Itzek, having a weight and height of about 5 T and 3.5 m, respectively. The experimental protocols were designed to involve the elephant in grasping tasks to test our hypotheses and to gather quantitative data without disturbing his daily life. We incorporated the experimental sessions into the elephant's daily routine with great care and attention. A thorough feasibility test was conducted prior to the study using mock objects to verify that the elephant's grasping behavior matched the observations made by Dagenais et al.[28] This approach was essential in facilitating the collection of dependable data throughout the study. Indeed, different exemplars may have individual variability in their grasping strategies.[52,53] Itzek had an open attitude to interact with unknown objects and scenarios. Hence, attracting the elephant's interest in the novelty of the scenario and using food as a reward were exploited to isolate and identify the interaction forces, and no prior training was performed. According to Jolly et al.,[54] the approach of animals to objects is the same as their approach to food, which is the best driver to initiate motion. An animal can differentiate between the smell of food and the objects involved in the measurements, and, consequently, it can manipulate the objects to reach food. The design of the protocol and the experimental setup were simplified as much as possible to facilitate potentially successful trials over the strict time window of the two weeks allowed for experimentation.

Table 1 summarizes our risk analysis.[55] The identified sources of risk are reported with the countermeasures and the probability (P), harm severity (H), and risk (R) scores.[56] P and H ranging from 1 (rare/very low) to 5 (highly probable/very high). R is the result of the product of P and H and is classified into minor ($R < 4$), moderate ($4 \leq R < 10$), major ($10 \leq R < 17$), and severe ($R > 17$). The average risk was calculated to decide whether the countermeasures would be sufficient.

In fact, elephants are more nervous or less likely to collaborate with humans when in musth, when the temperatures are too low, or when the weather is rainy. In any case, once the time window of the experiments was fixed, there were no effective countermeasures for musth.[57]

On the other hand, object breakage can be safely mitigated by the right choice of materials and by having replacements. Ingestion can be tackled by minimizing the possibility of the animal carrying/moving the objects outside the workspace. The main design guideline was to allow Itzek to safely insert his trunk inside the defined workspace without bringing any experimental object to his mouth. A battery was used to enable the sensorized object to work wirelessly, and the only event that could set off an explosion would have been if a battery had been dropped abruptly to the ground. In addition to an effective design for the sensorized objects, the risk can be considerably lowered by physically separating the animal from the explosion zone. Finally, food was the primary source of interest to keep his interest high.

Experimental setup and protocol

The setup consisted of the (4 × 1.5 × 2.5 m) box shown in Figure 1. The wall between the animal and the internal part of the box had an access point with a 30 cm diameter and 150 cm from the ground level. The size and thickness of the walls and the height of the openings from the ground were defined according to the size of the trunk, the animal's welfare, and the operators' safety. The back view of the working area, a 3D reconstruction of the setup, and two internal views are shown in Figure 1. Even though an elephant can operate in complex and unstructured scenarios, some constraints were needed to limit the variability in Itzek's response and to investigate individual aspects *per se*.

The experiments were designed to investigate the distal curling of the trunk, while introducing some sources of variability to encourage Itzek to use the pinching strategy. They were carried out to isolate as reasonably practicable the tactile sensibility of the trunk portion inserted in the workspace. Vision was occluded since the setup had only one open access point. Smell elicited and drove the elephant's attention: while the objects had the same neutral odor, food was placed inside cavities created on the ground floor, with dimensions such that the objects could fit on top of the food hidden below. Itzek was thus supposed to learn how to free the hole from the obstacle (sensorized object) and reach the food.

The experimental tasks were to pick and release two sensorized objects. The sensorized cylinder was placed with one support inside the dedicated ground hole and fixed by a rope the elephant could not access. This meant that Itzek would not have been able to throw the object far away or attempt to retrieve it from the workspace. He could grasp the object, lift it, and release it. In the experiment with the sensorized handle, Itzek had to extract the object from a ground hole. The handle had an internal cavity (which he could not access) to vary its weight (0 kg, 5 kg, and 10 kg). In contrast to the cylindrical object, the handle's initial ground position was changed throughout the trials (close, mid, and far).

Five Go Pro cameras recorded the experiments to follow the trunk motion at 120 Hz with 2.7 K resolution. Videos were temporally synchronized with force data and segmented to isolate trials and ease the analysis. The manual insertion of the specific object inside the ground hole was a source of variability. We observed that problems would arise if the cylinder got stuck or was too easy to move around.

Sensorized cylinder

The dimensions of the object and the distribution of the tactile elements were defined after an initial test with some not-sensorized mock-ups performed by the keepers. This way, a qualitative identification of the grasped area was addressed. The sensorized cylinder (see Figure 2A) comprises a modular case incorporating tactile sensors and an internal electronic board. All parts were custom designed to be robust and to provide reliable measurements in unconstrained scenarios. The case (height: 245 mm, ø: 49.2 mm, weight: 0.8 kg) is 3D printed (ProX6100 SLS, 3D Systems, 3DS-30103A) with DuraForm ProX PA. This plastic material is based on Nylon 11 and has excellent impact resistance and cyclic motion in harsh environments. The object has an internal case to host the electronic board and the battery. An inner foam lining facilitates the dumping of impacts, and openings are created to dissipate the heating from the electronics. The external case has two slots at the internal top and bottom parts to slide in and screw the inner part. The interior of the cylindrical wall is embossed to fit 10 flexible printed circuit boards (PCBs), which are positioned and then screwed. Each PCB integrates 8 coils, whose circular shape allowed correct routing of the PCB. On the other hand, the outer side of the cylinder wall has 80 circular slots to accommodate the elastomeric sensing taxels (Area: 3.65 cm^2), whose radial coordinates and shape are matched to the coils positioned in the above PCBs. The number of taxels was chosen as a trade-off between the spatial resolution and the complexity of the readout electronics.

The soft inductive taxels are based on the Eddy-current effect.[58,59] Each one comprises three-layered elements, i.e., a planar coil, a deformable layer, and a conductive film. Each coil is excited by a 0.1 MHz–10 MHz alternated current and generates an alternating magnetic field which induces an opposing magnetic field in the nearby conductive film. This magnetic field coupling reduces the inductance of the coil. A force applied on the sensing target displaces the conductive film toward the coil, thus decreasing the coupled inductance of the coil.

The elastomeric and conductive materials are discretized into mechanically separated taxels to reduce crosstalk

Ten configurations of the inductive sensors were tested using elastomers with different Young's Moduli; conductive layers with magnetic particles, and flexible 0.1 mm-thick ferrite films. All the combinations tested are reported in Table S1. They have a thickness of 6.5 mm, except for the Base one, which is 2 mm thick. A thickness of 2 mm is used as a reference, even though a soft layer with the required thickness would not transmit the force effectively in the final prototype (especially given the curved outer surface of the sensor).

The various sensors were characterized by means of an ad hoc indentation test apparatus. Each taxel is hosted on the top of a curved part that replicates the cylinder (same shape and material), by gluing with SilPoxy resin (Smooth-On, Inc.), whereas the corresponding PCB is fixed at the bottom part. This platform is positioned in an experimental set-up that has one orthogonal manual micrometric translation stage (M-105.10,

Physik Instrumente, Karl-sruhe, Germany) mechanically coupled with a micrometric servo-controlled translation stage (M-111.1DG, Physik Instrumente, Karlsruhe, Germany) equipped with a triaxial load cell (ATI Nano 17, ATI Industrial Automation, Inc., Apex, NC, USA).

A vertical force is exerted on the specific sample by means of a Delrin cylindrical probe interfaced with the load cell, whose dimension is equal to the area of the taxel. The inductance is read by a MyRIO-1950 (National Instruments, Austin, TX, USA). Each acquisition starts with the stage at the highest vertical position, while the hardware peripherals are initialized. The vertical position is controlled via software such that each acquisition begins at the same probe-taxel distance. The tests are performed for five cycles and 3 mm indentation depth.

Our results show that the taxels incorporating the ferrite sheet generally perform better than those with the MRE layer. Figure S5 also shows that stiffer top layers improved the sensing performance in terms of hysteresis, even though sensitivity is reduced. To counteract this lack of sensitivity, an additional ferrite sheet is integrated at the bottom, and a "softer" layer is used. As a result of this characterization phase, the sample F1FD (Ferrite-Ecoflex10-Ferrite-Dragonskin20) has the best configuration to be implemented in all the taxels.

The sensing measurements have high sensitivity for small stimuli, fast response, low hysteresis, and a full-scale output for each taxel higher than 15 N. Internal disturbances were rejected by adding an adhesive ferrite sheet on top of each PCB on the side facing the inner part of the cylinder, as shown in Figure 2A. In addition, shielded custom cables were fabricated to minimize further interferences. Once assembled, the device is ready to work. Figure 2B shows the overall system.

The soft inductive transduction method does not need the coil and the target layer to be physically attached, thus allowing all the electronic components to be inside the object. The 80 taxels are sampled by 20 LDC1614 chips (Texas Instruments, USA), one chip every 4 coils, and two chips sharing the same I2C line by setting different addresses. The 10 resulting I2C lines were multiplexed I2C to reach a sampling rate of 50 Hz. Tactile data, date/time data, and a 9-axis inertial data are streamed via Wi-Fi or logged onto an internal memory card. The device is powered by a battery (10 + h autonomy) with wired or wireless charging. As Figure 2C shows, sensors and peripherals are initialized at startup. Then there is an automatic transition to the Stop status unless an unrecoverable error is encountered (Error status).

While the board waits for user input, sensor data sampling is stopped. If no input is given, the board is put in low-power status. In run mode, each data sample is marked with a timestamp and contains the device orientation read from an IMU. The log files can be downloaded from the device using a Wi-Fi connection in the Dock status. It is possible to switch between the two modalities and change the configuration settings of the LDC1614 modules. In logging mode, the device acquisitions are started and stopped using a reed switch. The cylinder connects to a custom LabVIEW user interface (NI, National Instruments Corp.) that shows and saves data received as a user datagram protocol (UDP) stream while in streaming mode. A Boolean value can be triggered by pressing a button to highlight salient moments. Video S2 shows the cylinder operation and multiple views from one trial.

Sensorized handle

The sensorized handle (see Figure 3A) comprises a top part containing the electronics and the sensing components and an interchangeable bottom part to modulate the weight. As in the cylindrical object, these parts are built by 3D printing (ProX6100 SLS) of DuraForm ProX PA material.

The top part has two interlocking halves and is custom designed to have dimensions and affordance that induce the elephant to grasp it.[28] Each half-handle has three slots on the lateral side where force sensitive resistors (FSRs) (UX 402, Interlink Electronics) are conformed to the handle and glued. Moreover, parts built from soft material are integrated on top of the FSRs to modulate the force losses in the measurements as their dome-like structure is touched and compressed before the handle wall. This way, the receptive field of each sensor element is enlarged.

Each slot has a thin slot toward the internal part through which the connectors can be passed. In fact, the inner surface of the handle was embossed to position and screw six switchable voltage dividers (10340, Phidgets, Inc.). An additional embossing was made to place an Inertial Measurement Unit (IMU) BNO085 (Adafruit 9-DOF Orientation IMU Fusion Breakout). The connectors of the six voltage dividers and the IMU can go through two nozzles connecting the handle's internal part to the bottom surface, where they are connected to a microcontroller (Arduino Portenta H7, ABX00042). An internal cavity contains the power line on the opposite half of the handle to the microcontroller. The battery is secured inside an internal hole with a foam inner liner and opening to dissipate the heating. A cover protects both the electronics and the battery. The handle has a diameter of 42 mm at the level of the taxels and is 140 mm high. Each of the six taxels has an area of 8.25 cm^2. The base has a diameter of 300 mm, i.e., 20 mm wider than the weight holder. The base is 106 mm high and has a cylindrical guide to insert the weight and screw it to the top part.

Figure 3B shows how the internal components are connected and communicate. The board's architecture provides a maximum sampling rate of 150 Hz of 6 FSR, date/time, and a 9-axis IMU streamed via Wi-Fi. The device is powered by a rechargeable battery (10 + h autonomy). Figure 3C shows the state chart of the device. At startup, all the sensors and peripherals are initialized, and then there is an automatic transition to the pairing status unless an unrecoverable error is encountered (Error status). A custom LabVIEW user interface (NI, National Instruments Corp.) connects wirelessly to the handle in pairing mode. The interface commands the handle to start/stop streaming data and saves them to a file.

During an acquisition, each data sample is marked with a timestamp and contains the device orientation read from an IMU. In addition, critical moments can be highlighted by pressing a flag button. An ongoing data streaming is shown in Video S3. A Dragonskin (Smooth-On, Inc.) force condenser was fabricated to protect the FSR from direct contact and to modulate the force exerted on the taxels. The same indentation station used to characterize the sensorized cylinder was used here as well. An FSR was put on a hosting platform that replicated the handle, with the force condenser glued on top using SilPoxy resin (Smooth-On, Inc.). Figures 2D and 3D show the cylinder and handle

characterization results. The corresponding polynomial fittings have an r^2 equal to 0.993 and a root-mean-square error (RMSE) of 0.659 for the cylinder, and an r^2 value of 0.996 with an RMSE of 0.395 for the handle.

Data selection and cleaning

The whole experimental session consisted of three days of experiments with the sensorized cylinder and three days with the sensorized handle. An initial coarse classification was obtained by sequencing the videos to identify the trials from which data could potentially be gathered. This procedure resulted in 23 potential trials for the sensorized cylinder and 58 for the sensorized handle.

Then, raw force data were synchronized with the potential trials to check whether the specific trial could be chosen more accurately. Data were filtered with a 4th-order Chebyshev lowpass IIR filter with passband frequency at 5 Hz and passband ripple of 1E−3, using a zero-phase forward and reverse digital IIR filtering method. After filtering in the forward direction, the filtered data were reversed and run back through the filter. As a result, zero phase distortion was obtained, and the magnitude was modified by the square of the filter's magnitude response. The selection was made by using a MATLAB application to show different views of the experiments simultaneously, together with force data (see Video S1). This further selection left nine trials for the experiments with the cylinder, shown in Figure S1. Seven additional trials were added to analyze the contact area, even though they were not clean enough to be used for force-related processing. There were 25 selected trials for the handle, i.e., 9 for the proximal insertion point, 12 for the central insertion point, and 4 for the distal one. Figure S2 shows a subset of the trials for the experiments with the handle, grouped by object weight and location within the workspace. These trials were further preprocessed by identifying the time window in which the grasping and manipulation occurred. In both Figures S1 and S2, the white region of each graph shows the manipulation time, whereas the discarded parts of the data are in gray.

The spatial distribution of the applied forces was then analyzed when the maximum force was exerted by the trunk. For each trial, the 8x10 force mapping matrix was identified (see Figure S3B). The first image is used as the target, and all the others are aligned with that one. Each image is replicated three times in both the horizontal and the vertical direction, and then rotated at intervals of 5°. The cross-correlation between the rotated and repeated image and the target image at each rotation step is calculated. The selected image is the sub-image with the same dimensions as the target for which the cross-correlation is maximized. The maximum value corresponds to the roto-translation of the image that most matches the target image and compensates for the absence of controllability of the grasping point and orientation. Figure S3A shows an example of a target and base image and the result of the cross-correlation for some rotations of the replicated image.

QUANTIFICATION AND STATISTICAL ANALYSIS

Concerning the experiments with the cylinder, data underlying distribution was evaluated with the Kolmogorov-Smirnov test for time, force, contact area, and similarity, in compliance with its hypothesis of small sample size. The violin plots in Figures 4A, 4D, and 4E show that the actual distribution for force and contact area is not Gaussian. In fact, by repeating the normality test for a small sample size with Shapiro-Wilk, those two distributions failed to reject the null hypothesis. This discrepancy can be related to the number of trials. No further non-parametric analysis was performed since data were not supposed to be put into any relationship.

Concerning the experiments with the handle, the close and middle distribution cannot be compared solely through a statistical test since the weight represents a second parameter. In this regard, the number of trials is between 3 and 4 for each weight and for each position. It was not possible to obtain further data because of the time in which the authors were allowed to perform experiments with the animal, for his welfare. Hence, the statistical power of a two-way ANOVA (or Kruskal-Wallis for non-Gaussian distribution) would be too low. Still, these variables provide information on how the elephant grasped the object.